Solvent Desorption of Asphaltenes from Solid Surfaces

Lene TAPIO, Sreedhar SUBRAMANIAN, Sébastien SIMON*, Johan SJÖBLOM

Ugelstad Laboratory, Department of Chemical Engineering, Norwegian University of Science and Technology (NTNU), N-7491 Trondheim, Norway

ABSTRACT

The main goal of this paper is to compare the ability of different organic solvents to desorb asphaltenes from stainless steel surfaces. The asphaltenes were extracted from a North Sea crude oil by precipitation. The organic solvents are characterized based on their Hansen solubility parameters. The adsorption of asphaltenes was followed by means of a Quartz Crystal Microbalance with Dissipation (QCM-D). The asphaltene desorption efficiency of the solvents tested varied between 20% and 70%, with pyridine as the most efficient solvent. Carbon disulfide was found to be a poor desorption solvent, indicating the importance of solvent polarity. A simple model based on the Hansen solubility parameters of parameters seemed to give a good quantitative explanation of experimental desorption experiments.

Keywords:

Asphaltenes, Adsorption, Hansen Solubility Parameter, Desorption, QCM

* Corresponding author. Tel.: (+47) 73 59 16 57 Fax: (+47) 73 59 40 80

E-mail address: sebastien.simon@chemeng.ntnu.no

1. INTRODUCTION

A variety of problems occur in crude oil exploitation, transport and processing that can violate the regularity of the process. Normally this is related to a behavior described as flow assurance and separation. Flow assurance summarizes phenomena that can prevent the well fluids to be transported in pipes from a production site to a processing site. Since the transport can encompass large distances, large variations in temperature and pressure and different flow regimes, the most common phenomena to cause irregularities are plugging behavior originating from wax[1], asphaltenes[2-5] and gas hydrates[6] or combinations of these. The efficient mixing of the oil and water phases either in pipe or in separator is the background for an emulsion formation. The severity of this state is highly dependent on the composition of the crude oil phase and especially so on the existence of heavy and polar components. These molecules normally termed resins and asphaltenes are indigenous emulsion stabilizers[7-9] due to their accumulation at the w/o interface. The interfacial composition and properties will highly dictate the stability of the macroscopic emulsion state.

Asphaltenes are per definition the crude oil fraction which is insoluble in n-pentane but soluble in toluene or an organic solvent in general[10-12]. The molecular structure of asphaltenes gives rise to a molecular aggregation in the bulk phase especially so for aliphatic hydrocarbons and to a pronounced adsorption onto solid surfaces like pipe walls and solid rock formation[13-14]. In addition to their interfacial activity discussed above. Since the affinity of asphaltenes onto solid surfaces is attributed to their adsorption capacity, this is a good measure of their propensity to plug the pipe lines during transport.

In this study we used Quartz Crystal Microbalance with Dissipation (QCM-D) to study the adsorption of asphaltenes onto stainless steel surface, and also asphaltene desorption by

means of selected organic solvents. The results are explained by using the concept of Hansen solubility parameters (HSP).

2. EXPERIMENTAL SECTION

2.1. Chemicals

The solvents and chemicals used were of analytical grade, and were used with no further purification. They were obtained from Sigma-Aldrich (hexane (≥95%); Carbon disulfide (≥99.9%); Pyridine (99.8 %); Aniline (99 %), Quinoline (98 %)), VWR (Tetrahydrofuran (≥99.7%); Xylene (98.5 %); Ethanol (96%)), Merck (Chloroform (99.2 %)) and Hellma Analytics (Hellmanex III).

Asphaltenes were obtained from a chemical free North Sea crude oil using the following procedure. The crude oil was initially preheated in an oven to 60 °C for 2 hours. Thereafter, 16 g of crude oil was sampled and 640 ml of hexane was added to it. The oil mixture was stirred overnight at room temperature. The mixture was filtered under vacuum using 0.45µm HVLP filter (Millipore) and the asphaltenes obtained were washed with n-hexane until the filtrate was colourless. Finally, the asphaltenes were dried in a dessicator using nitrogen for at least 48 hours. The elemental composition of asphaltenes is given in table 1.

Element	Carbon	Hydrogen	Nitrogen	Oxygen	Sulfur
Composition (wt%)	85.6	8.17	1.32	1.85	1.96

Table 1: Elemental composition of asphaltenes[15]

2.2. Quartz Crystal Microbalance with Dissipation (QCM-D)

2.2.1. Theory

The quartz crystal microbalance (QCM) is a nanogram sensitive technique that measures the amount of substance adsorbed onto a coated crystal[16]. The quartz crystal oscillates at constant frequency when electric field is applied. When mass is adsorbed to the crystal, the resonance frequency changes. The mass adsorbed can be calculated from the change in frequency before and after adsorption, using the Sauerbrey equation[17]:

$$\Delta m = -\frac{\rho_q t_q}{n f_0}\Delta f = -\frac{C}{n}\Delta f \quad (1)$$

where Δm is the change in mass, t_q (≈ 0.3 mm) is the thickness of the quartz, ρ_q (= 2648 kg/m^3) is the density of the quarts, f_0 (= 5 MHz) is the fundamental frequency of the crystal, C is 0.177 mg/m^{2}Hz and n is the overtone number. A few conditions must be met for the Sauerbrey equation to be valid[17]:

- The adsorbed mass is distributed evenly on the crystal.
- Δm is much smaller than the mass of the crystal itself (<1%).
- The adsorbed mass is rigidly adsorbed to the crystal.

The QCM also measures dissipation, which provides information about the structure and viscoelasticity of the film. Dissipation is measured from the time it takes the oscillating crystal to slow down when the power is disconnected. The dissipation factor is proportional to the power dissipation in the oscillatory system[18]:

$$D = \frac{E_{dissipated}}{2\pi E_{stored}} \quad (2)$$

Where, $E_{dissipated}$ is the energy dissipated during one oscillation and E_{Stored} is the energy stored in the dissipating system. The change in dissipation (ΔD) before and after adsorption gives information about the viscoelasticity of the layer adsorbed. A change in dissipation of less than 10^{-6} indicates that the adsorbed layer is rigid, and higher ΔD values indicate a more viscoelastic layer[19].

2.2.2. Crystal cleaning protocol

Quartz crystals coated with stainless steel were used for the experiments. The composition of the stainless steel coating on quartz crystal can be found elsewhere[15]. The crystals were procured from Biolin Scientific (Sweden). Prior to use, the crystal was immersed in 1% hellmanex solution for at least one hour. Thereafter, it was rinsed with purified water and dried with nitrogen gas. The crystal was then sonicated for 10 min in ethanol, rinsed with purified water, dried with nitrogen gas and finally subjected to UV treatment for 15 min.

2.2.3. Asphaltene solution preparation

Three solutions of asphaltenes in xylene were prepared in 30 mL glass vials, with concentrations of 0.1 g/l, 0.5 g/l and 1.0 g/l. The samples were sonicated for 30 min after preparation to ensure that the asphaltenes were completely dissolved. If the samples were not used the same day, they were sonicated again for 10 min before starting the experiments.

2.2.4. QCM Measurements

A single sensor microbalance system Q-Sense E1 from Biolin Scientific (Sweden) was used for measurement. Stainless steel coated quartz crystal was placed inside the chamber of QCM. The temperature in the chamber was maintained at 20°C. Solutions of asphaltene and xylene were injected at a flowrate of 750µl/min for 10 min.

Initially, xylene was used to obtain a baseline. This was done by injecting xylene into the chamber for 10 min and waiting until the frequency was stable (i.e., ±1 Hz variation in 10 min) after injection. The adsorption of asphaltene started with injection of 0.1 g/l asphaltene solution, followed by injection of 0.5 g/l and 1.0 g/l asphaltene solutions. Thereafter, xylene

was injected to remove the loosely bound asphaltenes on the surface. Three sequences of selected solvent was then injected (the injected solvents are listed in Table 2). The injection of solvent (other than xylene) results in a significant shift in baseline since their density and bulk viscosity are different from xylene's. Hence xylene was once again injected at the end of the experiment to compensate for the baseline shift.

3. RESULTS AND DISCUSSION

3.1. Asphaltene adsorption

A typical plot obtained in a QCM experiment is shown in figure 1. The data is presented for 5^{th} overtone since the system was earlier found to be sensitive to bulk flow effects at 3^{rd} overtone.[15] The injection of xylene at the start of experiment provides the baseline. Thereafter, as 0.1 g/l asphaltene solution is injected, the frequency decreases due to adsorption of asphaltenes onto the stainless steel surface. Further injections of asphaltene solutions of higher concentrations (0.5 g/l and 1.0 g/l) do not result in further frequency decrease. This indicates that the surface of crystal has been saturated with asphaltenes[15, 20]. Similarly, the dissipation change observed on injection of asphaltene solutions is close to 10^{-6}, thereby indicating the formation of a highly rigid layer. Thus sauerbrey relationship (equation 1) is valid and can be used for the determination of mass adsorbed onto the surface.

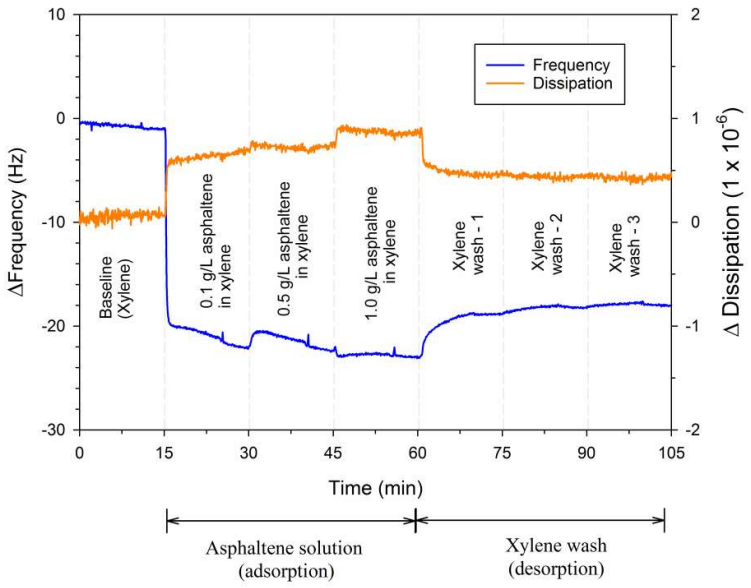

Figure 1: Asphaltene adsorption onto stainless steel based on 5th overtone

The xylene wash at the end of experiment has only limited efficiency in desorption of asphaltenes. On an average, only 22 ± 4 wt% of asphaltenes was desorbed from the stainless steel surface during xylene wash. The limited adsorption observed is consistent with the earlier results[15, 20] for asphaltenes precipitated from the same crude oil.

3.2. Asphaltene desorption with different solvents

Figure 2 gives a typical plot obtained when a second solvent (example THF) was used to induce desorption of asphaltenes. Injection of a second solvent after the first xylene wash results in significant shift in both the frequency and dissipation values. This is due to the fact that, in addition to desorption of asphaltenes and therefore a reduction of mass of the crystal, the density and bulk viscosity of the solvent injected differs from the xylene, and hence the baseline shifts. When xylene is injected again (xylene wash - 2) at the end of solvent wash, the baseline shifts back to correspond to the xylene baseline. Thus it is possible to now determine the amount of asphaltenes remaining on the stainless steel surface.

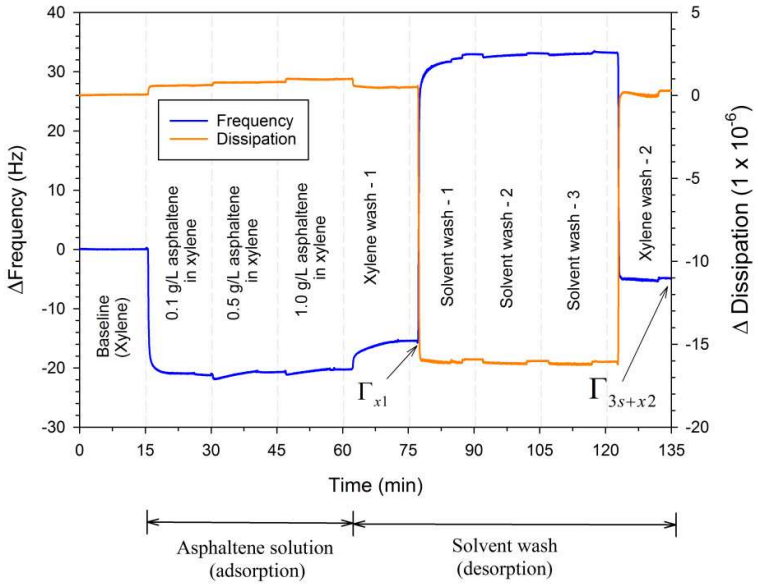

Figure 2: Example of asphaltene desorption using THF as solvent

The percentage of asphaltenes desorbed by the solvent after xylene wash is calculated based on equation 3.

$$wt\%\ asphaltenes\ desorbed\ by\ solvent = \frac{\Gamma_{x1} - \Gamma_{3s+x2}}{\Gamma_{x1}} \times 100 \qquad (3)$$

Where Γ_{x1} refers to the mass of asphaltenes remaining after xylene wash - 1 and Γ_{3s+x2} refers to the mass of asphaltenes remaining after 3 solvent washes and xylene wash - 2. Since the mass adsorbed is proportional to frequency change, the desorption efficiency in equation 3 can be calculated directly using frequency change (Δf) values.

To investigate whether there was any permanent shift in the baseline due to adsorption of solvent to the crystal when a second solvent was injected, experiments with only solvents and xylene were also conducted. In this case, xylene was used to find the baseline. After that, one of the solvents was injected, followed by injection of xylene again. The baseline shifted back

to normal (Δf = [-1 Hz, 1 Hz]) after the second injection of xylene and hence it was concluded that there was no permanent shift due to adsorption of solvent.

The values presented are the average of at least 2 parallels. It must be noted that some QCM experiments were not used as the asphaltene adsorbed amounts before or after the 1st xylene washing deviated significantly from other parallels (outliers). 3 experiments over a total of 19 were not considered in the following. These outliers were most likely due to contamination of crystals or due to the fact that the crystals have been used and washed with powerful cleaning solvents too often. As a consequence, new crystals were regularly used.

The comparison of desorption efficiency of different solvents is given in table 2. Among the solvents, pyridine exhibited the highest desorption efficiency (~70%) followed by chloroform (~58%). Aromatic solvents interact with the asphaltenes by replacing the π-π interactions among asphaltenes molecules thereby solubilizing them. Similarly, solvents with presence of heteroatoms and polar groups are expected to be good asphaltene dissolvers.[21] Even though carbon disulphide (CS_2) contains heteroatom sulfur, it was less effective in removing asphaltenes. This could be due to it being a non-polar solvent. Table 2 indicates that the solvent polarity plays an equally important role in effective asphaltene desorption.

Solvent	wt% asphaltene desorbed
Tetrahydrofuran (THF)	46.4 ± 1.7
Chloroform	58.4 ± 7.4
Pyridine	69.3 ± 8.8
Aniline	35.4 ± 0.9
Carbon disulfide (CS_2)	18.2 ± 2.7

Quinoline	52.3 ± 5.5

Table 2: Desorption efficiency of different solvents. The error bars represent the reproducibility.

3.3. Correlation between asphaltenes desorbed and Hansen solubility parameters (HSP)

3.3.1. Hansen solubility parameters

Solubility parameters allow us to predict if a substance will dissolve in another. A solid will most likely dissolve in a liquid with similar solubility parameters, and two liquids with similar solubility parameters tend to form a homogenous mixture.[22] The Hildebrand solubility parameter (δ) is defined by:

$$\delta = \sqrt{\frac{E}{v}} \tag{4}$$

Where, v and E refer to the molar volume and the cohesive energy density of the solute/solvent. The cohesive energy density consists of three types of interactions:

- Dispersion interactions (E_D) due to van der waals attractive forces
- Permanent dipole-permanent dipole interactions or polar cohesive energy (E_P)
- Hydrogen bonding (E_H)

The different contributions of cohesive energy densities add up to give the total cohesive energy density:

$$E = E_D + E_P + E_H \tag{5}$$

In terms of solubility parameters, equation 5 can be written as

$$\delta^2 = \delta_D^2 + \delta_P^2 + \delta_H^2 \tag{6}$$

The subscript D, P and H refer to the contribution of dispersion forces, polarity and hydrogen bonding components to the solubility parameter. An equation for solubility parameter distance (R_a) between two materials was developed by Skaarup[22] and is given by:

$$R_a = \sqrt{4\left(\delta_{D,1} - \delta_{D,2}\right)^2 + \left(\delta_{P,1} - \delta_{P,2}\right)^2 + \left(\delta_{H,1} - H_{D,2}\right)^2} \quad (7)$$

Where, subscripts 1 and 2 represent solute/solvent 1 and 2. A smaller R_a results in a higher solubility because the cohesive energy from the three sources is similar for the two substances.

Several studies have dealt with determining the solubility parameters of asphaltenes mostly using the solubility sphere method based on experimental determination of the solubility or non-solubility of asphaltenes in various solvents with known solubility parameters[23-25]. By reporting the solubility in a three dimensional coordinate system representing the three components of the Hansen solubility parameters, good solvents for asphaltenes are plotted to the interior of the sphere and poor solvents are outside the sphere. The centre of the sphere represents HSP of asphaltenes. The solubility is generally determined visually even if dynamic light scattering has also been used[23]. The HSP of asphaltenes varies according to their origin and therefore their composition[23], but seems to fall in narrow limits with $\delta_{D,asp}$ varying from 19.1 to 19.6 $MPa^{1/2}$, $\delta_{P,asp}$ from 3.4 to 4.7 $MPa^{1/2}$ and $\delta_{H,asp}$ from 4.2 to 4.4 $MPa^{1/2}$ [23-25]. Asphaltene fractions have different HSP than unfractionated asphaltenes[24]. Fossen et al.[26] used another method to determine the HSP for crude oils and SARA fractions including asphaltenes. They recorded the IR and NIR spectra for a set of solvents and binary solvents with various polarity and functional groups. Then they correlated the HSP to their respective IR and NIR spectra by multivariate analysis to build up a calibration curve. Due to this calibration, the HSP for crude oils and SARA fractions were determined by measuring their spectra. The values for asphaltenes from a set of 20 fractions vary from 15.0 to 15.8

MPa$^{1/2}$ for $\delta_{D,asp}$, 1.2 to 3.2 MPa$^{1/2}$ for $\delta_{P,asp}$ and 7.6 to 10.3 MPa$^{1/2}$ for $\delta_{H,asp}$.[26] Moreover, the authors indicated that the method could be improved by a better choice of calibration solvents.

3.3.2. Correlation between asphaltenes desorbed and Hansen solubility parameters

The Hansen solubility parameters of the solvents used in the study are given in table 3.

Solvent	Solubility Parameters (MPa$^{1/2}$)			Asphaltenes desorbed (wt%)
	δ_D	δ_P	δ_H	
Tetrahydrofuran (THF)	16.8	5.7	8.0	46.4
Chloroform	17.8	3.1	5.7	58.4
Pyridine	19.0	8.8	5.9	69.3
Aniline	19.4	5.1	10.2	35.4
Carbon disulfide (CS_2)	20.5	0	0.6	18.2
Quinoline	19.4	7.0	7.6	52.3

Table 3: Hansen solubility parameters (HSP) of solvents taken from Hansen[22] and amount of asphaltene desorbed by the solvent.

The HSP of the solvents with the corresponding asphaltene desorption (from table 3) can be visualized in a 3D bubble plot as shown in figure 3. The size of the bubbles is proportional to the asphaltenes desorbed.

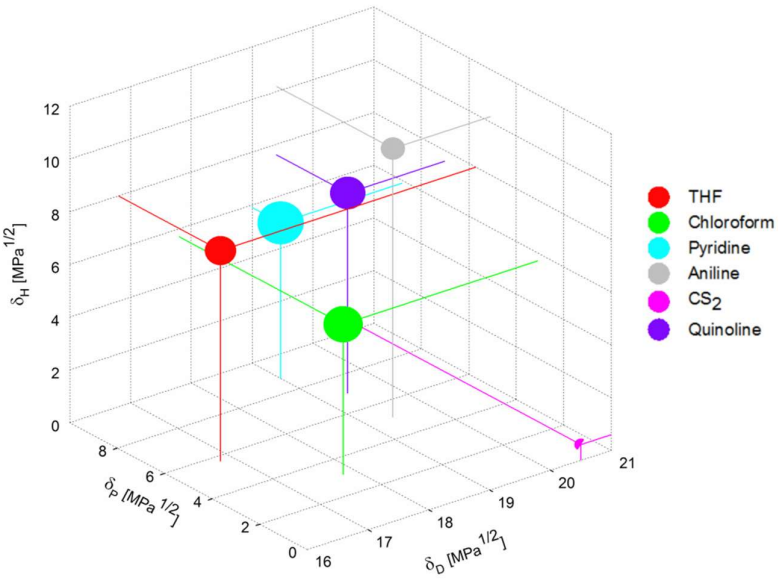

Figure 3: 3D bubble plot of HSP for solvents and desorption by solvents.

As mentioned earlier in section 3.3.1, the HSP distance (R_a) gives information of how well a solvent can dissolve a substance. Therefore a model (equation 8) is proposed based on the HSP distance, suggesting a linear relationship between the percentage of asphaltene remaining after adsorption (P_r) and HSP distance (R_a) between the solvent and the asphaltenes.

$$P_r \approx K \cdot \sqrt{4\left(\delta_{D,asp} - \delta_{D,sol}\right)^2 + \left(\delta_{P,asp} - \delta_{P,sol}\right)^2 + \left(\delta_{H,asp} - \delta_{H,sol}\right)^2} \qquad (8)$$

Where K is a constant, and the subscripts *asp* and *sol* refer to asphaltenes and solvent respectively. In order to estimate the HSP values of asphaltenes, the equation 8 was minimized to give the best fit. Thus the following HSP were obtained for asphaltenes: $\delta_{D,asp}$ = 18.6 $MPa^{1/2}$, $\delta_{P,asp}$ = 6.6 $MPa^{1/2}$and $\delta_{H,asp}$ = 3.9 $MPa^{1/2}$. The constant K = 9.8 minimized the equation 8. The model fits perfectly for all solvents except quinoline as shown in figure 4. The model predicts that asphaltene desorption using quinoline should be around 8% higher than experimentally observed. However, considering the accuracy of measurements (the

reproducibility is given in table 1), the model gives excellent prediction for THF, aniline and CS_2 while the fit is within the experimental deviation values for chloroform and pyridine. It can be noticed that the HSP determined in this article from desorption measurements are close (even if $\delta_{P,asp}$ is higher) to the ones determined from solubility measurements and summarized in section 3.3.1. This similarity is consistent: a good solvent would tend to induce the desorption of more asphaltenes even if specific interactions between asphaltenes and solid surface must be taken into account.

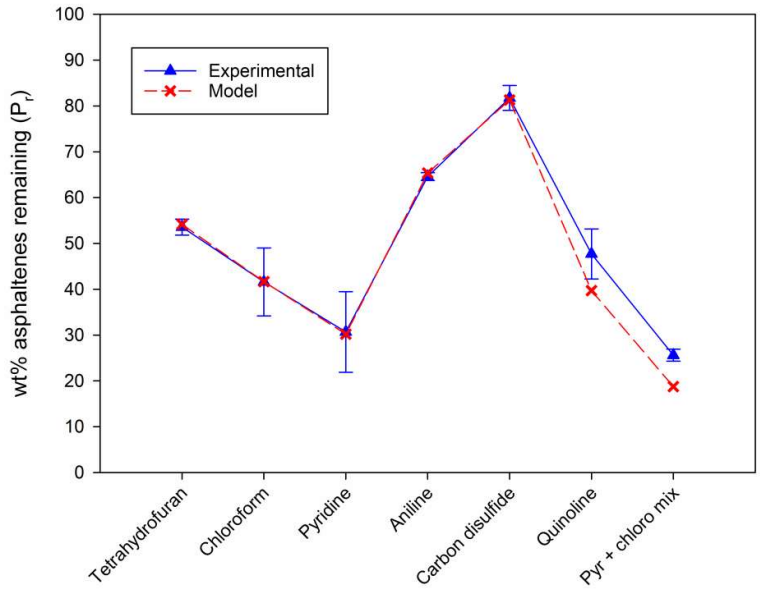

Figure 4: Fitting of model (equation 8) to asphaltene desorption ability of solvents and validation of model. 'Pyr + chloro mix' refers to mixture of pyridine (60 vol%) and chloroform (40 vol%).

In order to validate the model, a mixture of solvents pyridine (60 vol%) and chloroform (vol%) was selected. The solubility parameter of the solvent mixture was calculated based on equation 9.

$$\delta_i = \phi_{pyridine}\delta_{i,pyridine} + \phi_{chloroform}\delta_{i,chloroform} \quad (9)$$

Where, subscript *i* represents the three partial interactional forces (dispersion D, polarity P and hydrogen bonding H) and ϕ refers the volume fraction. Thus the calculated solubility parameters of pyridine (60 vol%) + chloroform (40 vol%) mixture was: $\delta_{D,\,mix}$ = 18.5 MPa$^{1/2}$, $\delta_{P,mix}$ = 6.5 MPa$^{1/2}$and $\delta_{H,mix}$ = 5.8 MPa$^{1/2}$ (The subscript *mix* refers to solvent mixture). The solvent mixture has HSP closer to the asphaltenes and is hence expected to be more efficient in desorption. The model (equation 8) predicted that use of this solvent mixture will result in desorption of 79 wt% of asphaltenes (or P_r = 21 wt%).

Figure 4 shows the model validation for solvent system with pyridine (60 vol%) and chloroform (40 vol%) mixture included. The experimentally determined amount of asphaltenes remaining after desorption using solvent mixture was 25.6 ± 1.2 wt%. The experimental value is close to the model predicted value (21 wt%) , thus validating the ability of model to predict the desorption capabilities of pure solvents as well as solvent mixtures.

4. CONCLUSION

A selection of solvents was tested to desorb asphaltenes from a stainless steel surface. Of the solvents tested (THF, chloroform, pyridine, aniline, CS_2 and quinoline), pyridine gave the highest asphaltene desorption, with an average desorption of 70% (by weight). The non-polar CS_2 was the least effective with an average desorption of only 18% (by weight), thereby indicating the importance of solvent polarity in effective asphaltene desorption. The Hansen solubility parameters (HSP) of the asphaltenes ($\delta_{D,asp}$ = 18.6 MPa$^{1/2}$, $\delta_{P,asp}$ = 6.6 MPa$^{1/2}$, and $\delta_{H,asp}$ = 3.9 MPa$^{1/2}$) were estimated using a model, which is also capable of predicting the desorption capability of solvents. The proposed model was validated for a binary solvent mixture and was found to be robust.

5. ACKNOWLEDGEMENT

The authors thank JIP Asphaltene consortium “Improved Mechanism of Asphaltene Deposition, Precipitation and Fouling to Minimize Irregularities in Production and Transport (NFR PETROMAKS)”, consisting of Ugelstad Laboratory (NTNU, Norway), University of Alberta (Canada), University of Pau (France), Universidade Federal do Paraná (Brazil) and funded by Norwegian Research Council (Grant no. 234112) and the following industrial sponsors – AkzoNobel, BP, Canada Natural Resources, Nalco Champion, Petrobras, Statoil and Total E&P Norge AS.

6. REFERENCES

1. Aiyejina, A.; Chakrabarti, D. P.; Pilgrim, A.; Sastry, M. K. S. Wax formation in oil pipelines: A critical review. *International Journal of Multiphase Flow* **2011,** *37* (7), 671-694.

2. Shokrlu, Y. H.; Kharrat, R.; Ghazanfari, M. H.; Saraji, S. Modified Screening Criteria of Potential Asphaltene Precipitation in Oil Reservoirs. *Petroleum Science and Technology* **2011,** *29* (13), 1407-1418.

3. Kleinitz, W.; Andersen, S. I. Asphaltene precipitates in oil production wells. *Oil Gas European Magazine* **1998**.

4. Thawer, R.; Nicoll, D. C.; Dick, G. Asphaltene deposition in production facilities. *Spe production engineering* **1990,** *5* (04), 475-480.

5. Wiehe, I. A.; Kennedy, R. J. The oil compatibility model and crude oil incompatibility. *Energy & fuels* **2000,** *14* (1), 56-59.

6. Sloan, E. D. Fundamental principles and applications of natural gas hydrates. *Nature* **2003,** *426* (6964), 353-363.

7. Spiecker, P. M.; Gawrys, K. L.; Trail, C. B.; Kilpatrick, P. K. Effects of petroleum resins on asphaltene aggregation and water-in-oil emulsion formation. *Colloids and surfaces A: Physicochemical and engineering aspects* **2003,** *220* (1), 9-27.

8. McLean, J. D.; Kilpatrick, P. K. Effects of asphaltene aggregation in model heptane–toluene mixtures on stability of water-in-oil emulsions. *Journal of Colloid and Interface Science* **1997,** *196* (1), 23-34.

9. McLean, J. D.; Kilpatrick, P. K. Effects of asphaltene solvency on stability of water-in-crude-oil emulsions. *Journal of Colloid and Interface Science* **1997,** *189* (2), 242-253.

10. Sjöblom, J.; Aske, N.; Auflem, I. H.; Brandal, Ø.; Havre, T. E.; Sæther, Ø.; Westvik, A.; Johnsen, E. E.; Kallevik, H. Our current understanding of water-in-crude oil emulsions.: Recent characterization techniques and high pressure performance. *Advances in Colloid and Interface Science* **2003,** *100*, 399-473.

11. Sjöblom, J.; Simon, S.; Xu, Z. Model molecules mimicking asphaltenes. *Advances in colloid and interface science* **2015,** *218*, 1-16.

12. Speight, J. Petroleum Asphaltenes-Part 1: Asphaltenes, resins and the structure of petroleum. *Oil & gas science and technology* **2004,** *59* (5), 467-477.

13. Dudášová, D.; Flåten, G. R.; Sjöblom, J.; Øye, G. Study of asphaltenes adsorption onto different minerals and clays: Part 2. Particle characterization and suspension stability. *Colloids and Surfaces A: Physicochemical and Engineering Aspects* **2009,** *335* (1), 62-72.

14. Adams, J. J. Asphaltene adsorption, a literature review. *Energy & Fuels* **2014,** *28* (5), 2831-2856.

15. Subramanian, S.; Simon, S.; Gao, B.; Sjöblom, J. Asphaltene fractionation based on adsorption onto calcium carbonate: Part 1. Characterization of sub-fractions and QCM-D measurements. *Colloids and Surfaces A: Physicochemical and Engineering Aspects* **2016,** *495*, 136-148.

16. Dixon, M. C. Quartz crystal microbalance with dissipation monitoring: enabling real-time characterization of biological materials and their interactions. *J Biomol Tech* **2008,** *19* (3), 151-158.

17. Sauerbrey, G. Verwendung von Schwingquarzen zur Wägung dünner Schichten und zur Mikrowägung. *Zeitschrift für physik* **1959,** *155* (2), 206-222.

18. Rodahl, M.; Höök, F.; Krozer, A.; Brzezinski, P.; Kasemo, B. Quartz crystal microbalance setup for frequency and Q-factor measurements in gaseous and liquid environments. *Review of Scientific Instruments* **1995,** *66* (7), 3924-3930.

19. Ekholm, P.; Blomberg, E.; Claesson, P.; Auflem, I. H.; Sjöblom, J.; Kornfeldt, A. A quartz crystal microbalance study of the adsorption of asphaltenes and resins onto a hydrophilic surface. *Journal of colloid and interface science* **2002,** *247* (2), 342-350.

20. Nenningsland, A. L.; Simon, S.; Sjöblom, J. Influence of Interfacial Rheological Properties on Stability of Asphaltene-Stabilized Emulsions. *Journal of Dispersion Science and Technology* **2014,** *35* (2), 231-243.

21. Kelland, M. A. Asphaltene Control. In *Production Chemicals for the Oil and Gas Industry*; CRC Press: Boca Raton, FL, 2009.

22. Hansen, C. M. *Hansen Solubility Parameters: A User's Handbook CRC Press*. *Boca Raton, FL* **2000**.

23. Sato, T.; Araki, S.; Morimoto, M.; Tanaka, R.; Yamamoto, H. Comparison of Hansen Solubility Parameter of Asphaltenes Extracted from Bitumen Produced in Different Geographical Regions. *Energy & Fuels* **2014,** *28* (2), 891-897.

24. Acevedo, S.; Castro, A.; Vásquez, E.; Marcano, F.; Ranaudo, M. a. A. Investigation of physical chemistry properties of asphaltenes using solubility parameters of asphaltenes and their fractions A1 and A2. *Energy & Fuels* **2010,** *24* (11), 5921-5933.

25. Redelius, P. G. The structure of asphaltenes in bitumen. *Road Materials and Pavement Design* **2006,** *7* (sup1), 143-162.

26. Fossen, M.; Hemmingsen, P. V.; Hannisdal, A.; Sjöblom, J.; Kallevik, H. Solubility Parameters Based on IR and NIR Spectra: I. Correlation to Polar Solutes and Binary Systems. *Journal of Dispersion Science and Technology* **2005,** *26* (2), 227-241.